Importance of nuclear models and Monte Carlo tools for radiation effects simulations

Rubén García Alía (CERN, R2E project)

Workshop for Applied Nuclear Data Activities (WANDA 2022) [FINAL]

28 Feb 2022, 07:30 → 4 Mar 2022, 18:15 US/Pacific

https://conferences.lbl.gov/event/880/

CERN R2E FLUKA G4SEE

Importance and use of Monte Carlo codes for accelerator R2E applications

- Simulation of the radiation environment
- Simulation of the radiation effects on electronics
  - Semi-empiric approach though SEE models combining technological information and free parameter(s) fitted to experimental data
  - Convolution of energy deposition distribution and response function, through RPP, nested RPP or IRPP
  - Main motivation of radiation effects simulation: **very broad range of particles and energies present in the accelerator mixed-field environment**

High-energy hadron environment in accelerators

SKORDIS, Eleftherios, et al. Impact of beam losses in the LHC collimation regions. 2015.

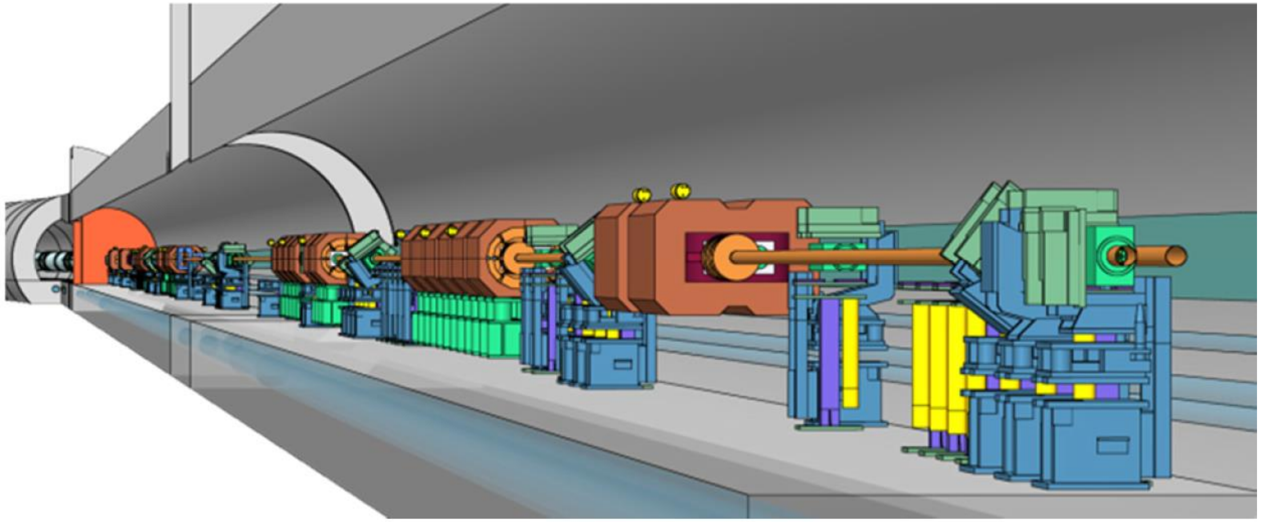

Figure 1: FLUKA model of the IR7 warm section.

- Importance of Monte Carlo codes (and radiation detectors) to assess radiation levels in high-energy accelerators

High-energy hadron environment in accelerators

K. Roeed et al., "Method for Measuring Mixed Field Radiation Levels Relevant for SEEs at the LHC," in IEEE Transactions on Nuclear Science, vol. 59, no. 4, pp. 1040-1047, Aug. 2012, doi: 10.1109/TNS.2012.2183677.

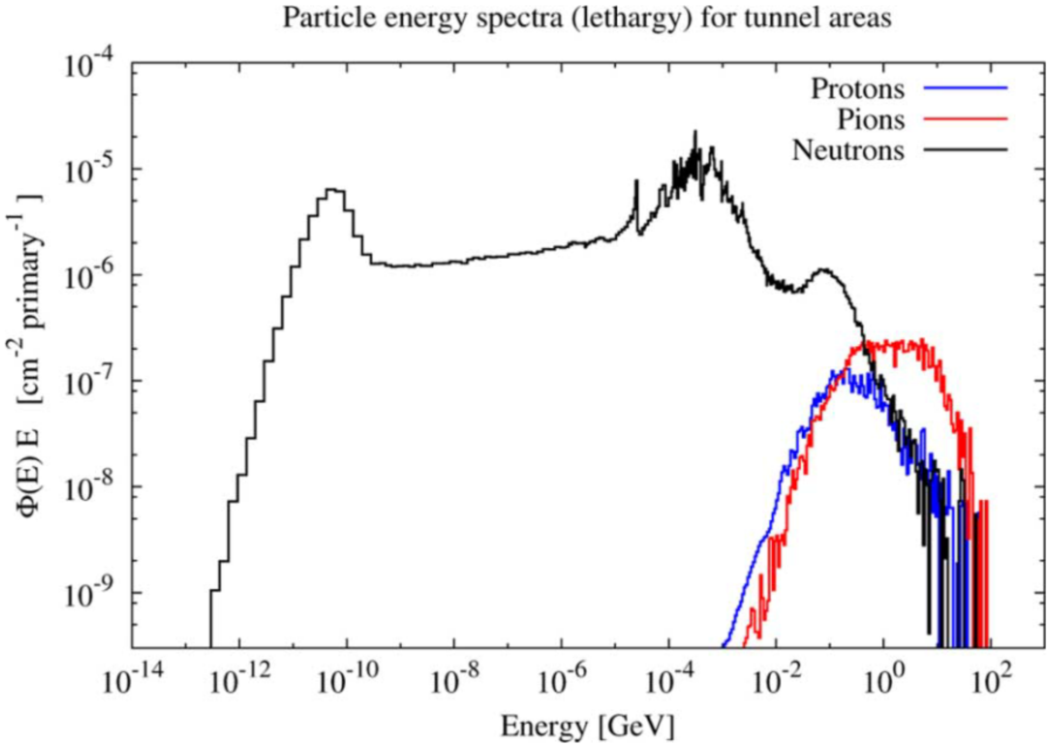

Fig. 1. Example of the simulated particle energy spectra (lethargy) representative for tunnel areas in the LHC. The radiation is due to particle debris induced by the colliding beams in one of the experiment points at CERN. The spectra is therefore normalized to one proton–proton collision (referred to as a primary in the y-axis label).

- Broad range of particle species (protons, pions, neutrons) and energies (from meV to GeV) that can cause disruption in electronic components and systems, notably through Single Event Effects

Typical SEE experimental data for R2E applications

- (Quasi-)Monoenergetic:
  - High-energy (20-200 MeV) protons at PSI
  - Intermediate energy (0.2-20 MeV) neutrons at PTB
  - Thermal neutrons (~25 meV) at ILL
- Spectra/mixed-field:
  - Spallation neutrons at ChipIr (from 800 MeV protons)
  - Mixed hadron field at CHARM (from 24 GeV protons)
- Mainly on SRAMs of different technology nodes (40-400nm), for both SEU and SEL

Introduction to slides on simulated and experimental SEE cross sections

- Taken directly from referenced publications
- Short comments related the main observations are included, but please check the papers for more details
- Comparisons between simulated and experimental SEE data should *not* be considered as physical benchmarks, as simulated SEE response depends on a variety of input parameters subject to large levels of uncertainty (e.g. component geometry and materials, SEE response function, etc.)
- However, these comparisons can be useful to spot significant deviations from experimental data for well calibrated semi-empirical models, as well as to compare results from different Monte Carlo codes and/or nuclear models

High-energy (>20 MeV) hadrons (protons, neutrons and pions)

R. García Alía et al., "SEU Measurements and Simulations in a Mixed Field Environment," in IEEE Transactions on Nuclear Science, vol. 60, no. 4, pp. 2469-2476, Aug. 2013, doi: 10.1109/TNS.2013.2249096.

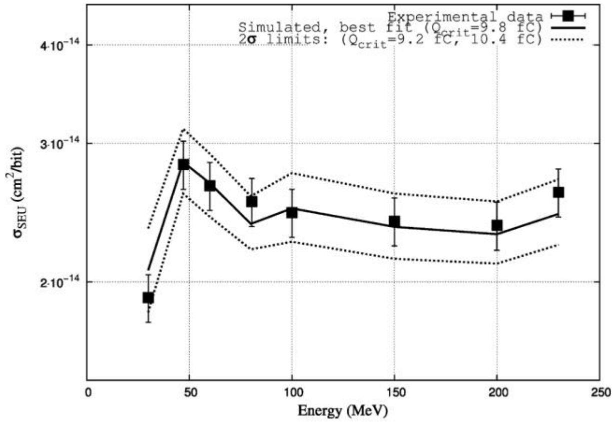

Fig. 4. Proton SEU cross section data for the ESA Monitor as a function of energy together with the corresponding simulated curve for the best fit of the critical charge to the data. Uncertainties in the data correspond to a 5% instrumental error associated to the fluence measurement at the test facility, and the count statistics for each cross section value. Uncertainties for the simulated cross section curve are taken as 2σ from the fit to the critical charge parameter and represented as dashed lines.

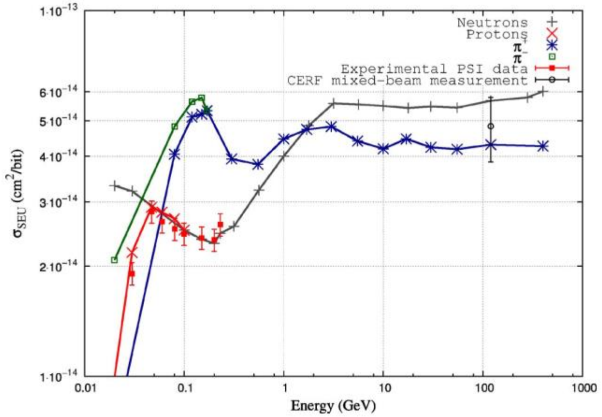

Fig. 5. Simulated proton, neutron and $\pi^{\pm}$ cross section for a sensitive volume of 0.25 μm^3 and a critical charge of 9.8 fC together with the experimental data used for the calibration of the model (also in Fig. 4 with a smaller energy range) and an experimental point at 120 GeV/c. The 2σ error associated to the fit of the critical charge is not explicitly shown to avoid overloading the graph, but is of $\sim \pm$ 15% for the different hadrons and energy values, similar to those represented in Fig. 4.

- Fairly constant proton SEU cross section in 50-230 MeV range, and rapid fall off at lower energies (strong dependence on package, lid, etc.)
- Neutron and proton equivalence above ~50 MeV
- Pion resonance at ~200 MeV
- Factor ~2 increase in SEU cross section between tens of MeV and hundreds of GeV, i.e. relatively constant with energy over many decades

More on pions

A. Coronetti et al., "The Pion Single-Event Effect Resonance and its Impact in an Accelerator Environment," in IEEE Transactions on Nuclear Science, vol. 67, no. 7, pp. 1606-1613, July 2020, doi: 10.1109/TNS.2020.2978228.

- More recent pion resonance SEU study, including also simulations for kaons

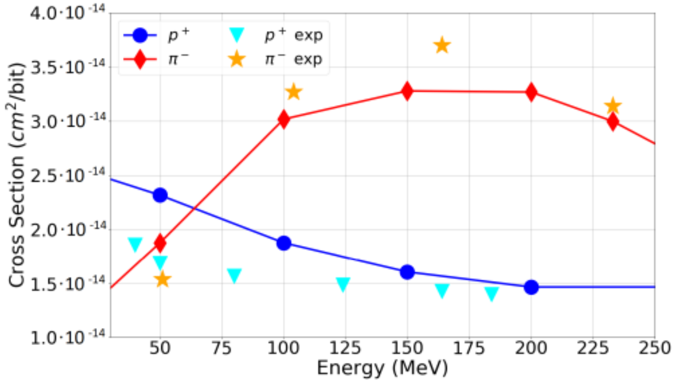

Fig. 9. Simulated cross sections for protons and negative pions and comparison with experimental data for the ISSI memory.

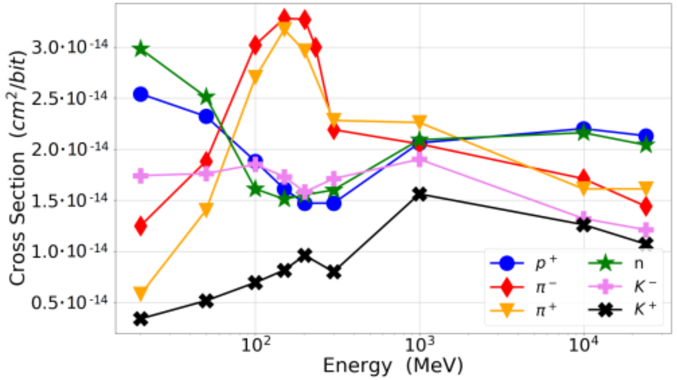

Fig. 10. Simulated cross sections for protons, charged pions, neutrons, and charged kaons over typical CHARM energy distributions for an RPP with 310-nm side and 0.75-fC critical charge.

More on pions

A. Coronetti et al., "The Pion Single-Event Latch-Up Cross Section Enhancement: Mechanisms and Consequences for Accelerator Hardness Assurance," in IEEE Transactions on Nuclear Science, vol. 68, no. 8, pp. 1613-1622, Aug. 2021, doi: 10.1109/TNS.2021.3070216.

- SEE cross section excess for pions also observed for SEL, extending down to lower energies

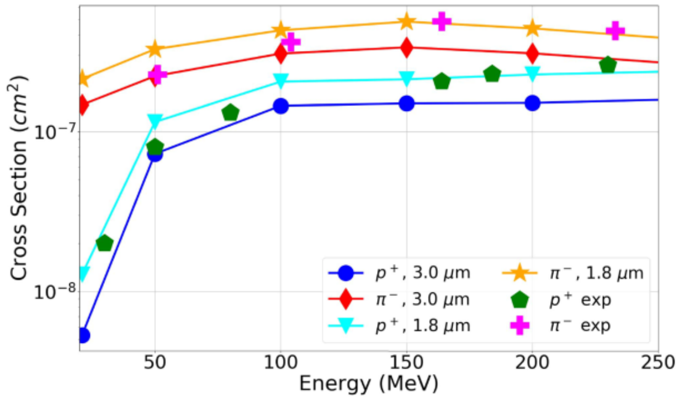

Fig. 5. Proton and negative pion SEL cross sections simulated with FLUKA for an SV thickness of 3.0 and 1.8 μm and compared to the Brilliance experimental data.

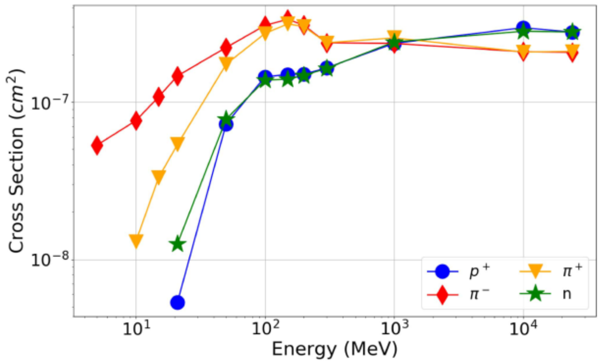

Fig. 6. FLUKA-simulated SEL cross sections as a function of energy for protons, charged pions, and neutrons. The energy range is meant to cover that of the CHARM facility.

Low energy protons

A. Coronetti *et al.*, "Assessment of Proton Direct Ionization for the Radiation Hardness Assurance of Deep Submicron SRAMs Used in Space Applications," in *IEEE Transactions on Nuclear Science*, vol. 68, no. 5, pp. 937-948, May 2021, doi: 10.1109/TNS.2021.3061209.

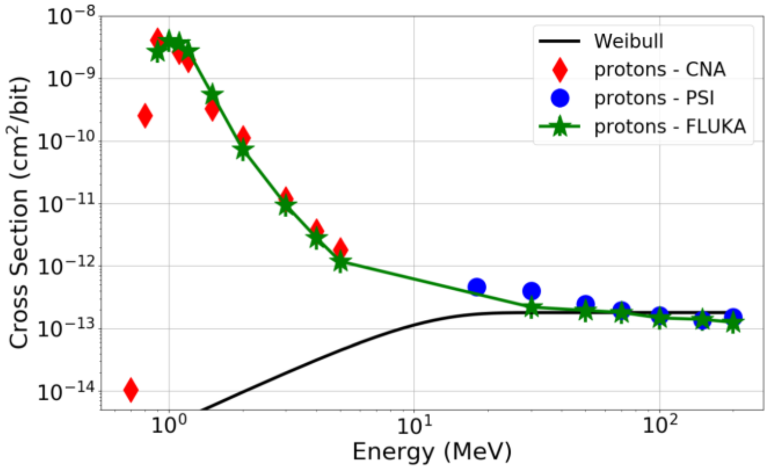

Fig. 1. Low and HEP experimental cross sections as a function of proton energy for the RADSAGA 65-nm SRAM when tuned at 0.3 V. The HEP data are fit with a Weibull with the following parameters: $\sigma_{sat} = 1.8 \times 10^{-13}$ cm^2/bit, $E_0 = 0$ MeV, $W = 10$ MeV, $s = 1.8$. The data are compared with the FLUKA simulated cross sections.

- Direct ionization from low energy protons meant that SEU cross section fall off at several tens of MeV no longer applies

Proton SEU contribution

Coronetti, Andrea. "Relevance and guidelines of radiation effect testing beyond the standards for electronic devices and systems used in space and at accelerators." *JYU dissertations* (2021).

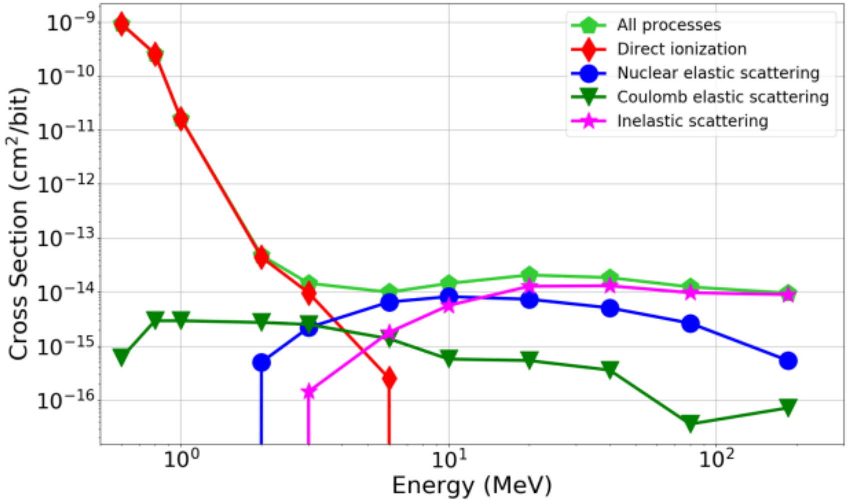

Figure 5.12: Proton SEU cross-section of various interaction mechanisms as a function of the primary proton energy for the ISSI SRAM. Obtained with G4SEE.

- Elastic scattering (Coulomb + nuclear) suppressed by direct ionization at low energies, and inelastic reactions at high energies

High-Z materials

R. G. Alía et al., "SEL Cross Section Energy Dependence Impact on the High Energy Accelerator Failure Rate," in IEEE Transactions on Nuclear Science, vol. 61, no. 6, pp. 2936-2944, Dec. 2014, doi: 10.1109/TNS.2014.2356641.

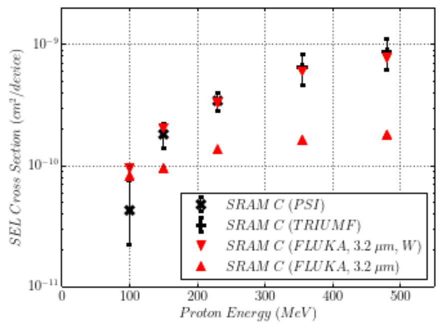

Fig. 6: SEL model output for SRAM C and a case without and with tungsten (labeled as *W*, and corresponding to a volume of 0.48 μm^3/cell) together with the PSI proton SEL data to which is was calibrated (100-230 MeV range) and TRIUMF SEL data in a larger energy interval (230-480 MeV). Measurements were performed at room temperature and a voltage bias of 3.3V.

- When high-Z materials are present near the sensitive volume of the components, effects with relatively large LET threshold will have a strong cross section increase with energy, between ~100 MeV and ~3 GeV

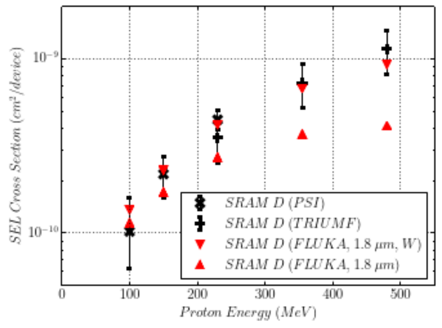

Fig. 7: SEL model output for SRAM D and a case without and with tungsten (labeled as *W*, and corresponding to a volume of 0.48 μm^3/cell) together with the PSI proton SEL data to which is was calibrated (100-230 MeV range) and TRIUMF SEL data in a larger energy interval (230-480 MeV). Measurements were performed at room temperature and a voltage bias of 3.3V.

High-Z materials

R. García Alía et al., "SEL Hardness Assurance in a Mixed Radiation Field," in IEEE Transactions on Nuclear Science, vol. 62, no. 6, pp. 2555-2562, Dec. 2015, doi: 10.1109/TNS.2015.2477597.

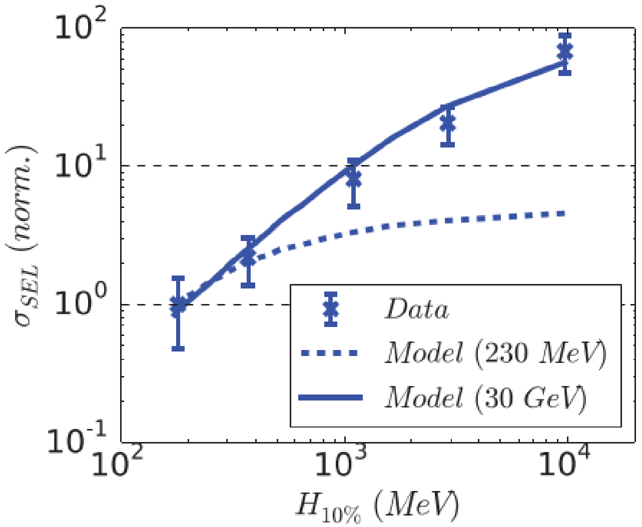

Fig. 11. Experimental mixed-field SEL cross section for SRAM C as a function of the 10% hardness energy normalized to the value at TL1 in CHARM. The expected SEL cross section from the models saturated at 230 MeV and considering the energy dependence up to 30 GeV are also shown.

- When high-Z materials are present near the sensitive volume of the components, effects with relatively large LET threshold will have a strong cross section increase with energy, between ~100 MeV and ~3 GeV

High-Z materials

R. García Alía et al., "SEE Testing in the 24-GeV Proton Beam at the CHARM Facility," in IEEE Transactions on Nuclear Science, vol. 65, no. 8, pp. 1750-1758, Aug. 2018, doi: 10.1109/TNS.2018.2829916.

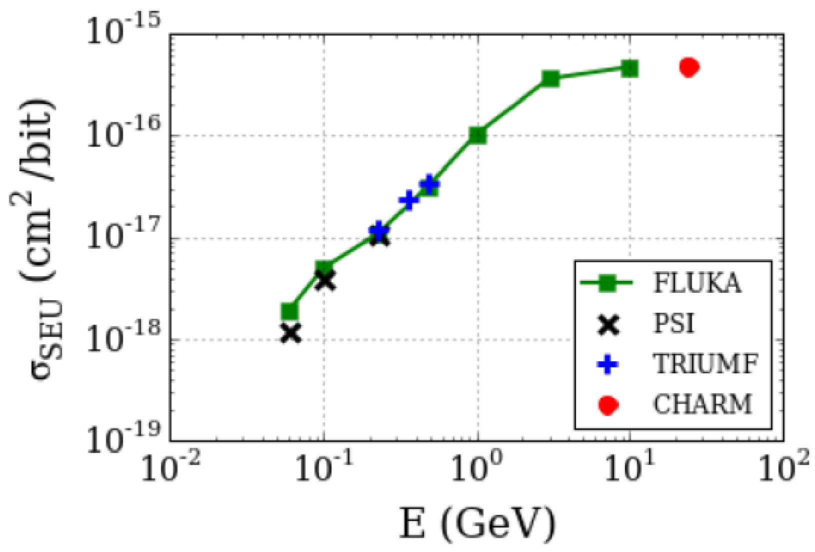

Fig. 8. Measured and simulated proton SEU cross section for Device B as a function of energy. More information about the rest of the mono-energetic data shown can be found in [14].

- When high-Z materials are present near the sensitive volume of the components, effects with relatively large LET threshold will have a strong cross section increase with energy, between ~100 MeV and ~3 GeV

High-Z materials

S. Uznanski et al., "The Effect of Proton Energy on SEU Cross Section of a 16 Mbit TFT PMOS SRAM with DRAM Capacitors," in IEEE Transactions on Nuclear Science, vol. 61, no. 6, pp. 3074-3079, Dec. 2014, doi: 10.1109/TNS.2014.2368150.

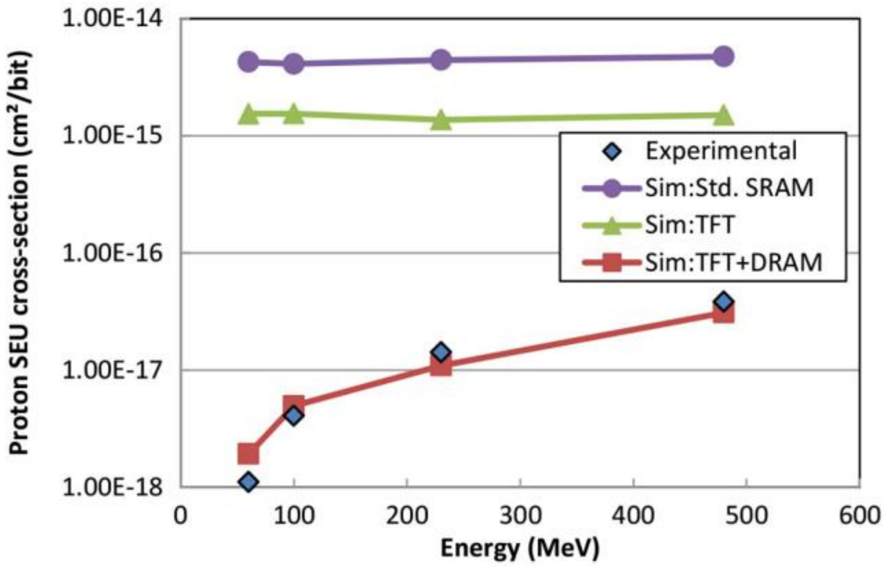

Fig. 6. Experimental data compared to the simulated proton SEU cross sections as a function of energy for a BEOL composed of SiO_2 and W layer and for different critical charge values corresponding to a standard SRAM (10 fC), TFT technology (26 fC), and TFT+DRAM technology (66 fC).

- When high-Z materials are present near the sensitive volume of the components, effects with relatively large LET threshold will have a strong cross section increase with energy, between ~100 MeV and ~3 GeV

Intermediate (0.2-20 MeV) energy neutrons

M. Cecchetto et al., "0.1–10 MeV Neutron Soft Error Rate in Accelerator and Atmospheric Environments," in IEEE Transactions on Nuclear Science, vol. 68, no. 5, pp. 873-883, May 2021, doi: 10.1109/TNS.2021.3064666.

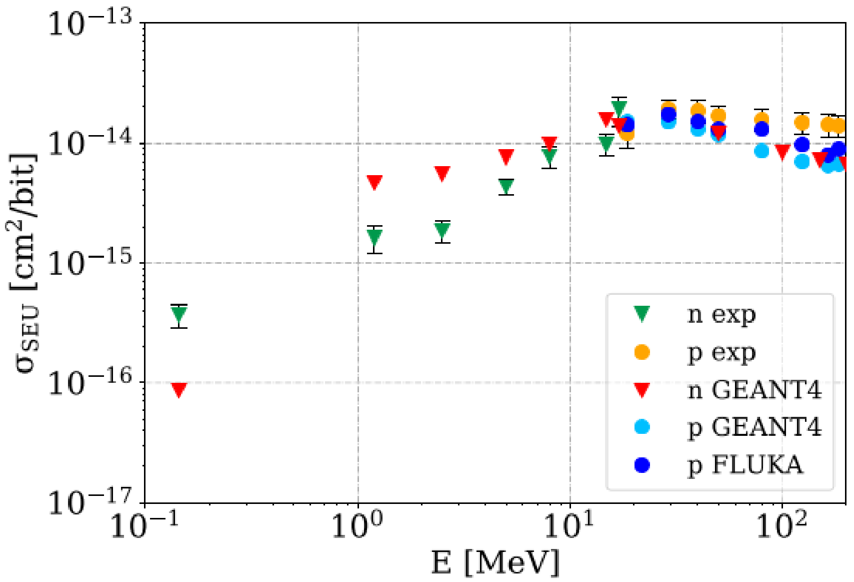

Fig. 11. ISSI 40 nm proton (p) and neutron (n) simulations and experimental data comparison. Proton simulations derive from FLUKA and GEANT4 tools, while the neutron ones from the latter.

- Importance of soft error contribution from intermediate (0.1-20 MeV) energy neutrons, particularly for components with low critical charges, and sensitive to proton direct ionization (i.e. (n,p) reactions, hydrogen recoils)

High-Energy Electrons

M. Tali et al., "Mechanisms of Electron-Induced Single-Event Latchup," in IEEE Transactions on Nuclear Science, vol. 66, no. 1, pp. 437-443, Jan. 2019, doi: 10.1109/TNS.2018.2884537.

M. Tali et al., "Mechanisms of Electron-Induced Single-Event Upsets in Medical and Experimental Linacs," in IEEE Transactions on Nuclear Science, vol. 65, no. 8, pp. 1715-1723, Aug. 2018, doi: 10.1109/TNS.2018.2843388.

- High-energy electrons (up to 200 MeV) can cause SEU and SEL even in relatively large LET threshold components, through photo-nuclear and electro-nuclear reactions, and with SEE cross sections that are a few orders of magnitude lower than for hadrons

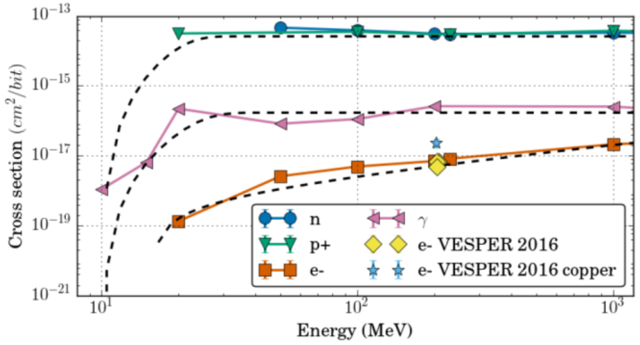

Fig. 11. Simulated cross-sections for the ESA SEU monitor. Measurements are shown, run with copper plate marked. Parameters of the Weibull fits can be seen in Table I. Weibull fits are shown with stippled lines. [8]

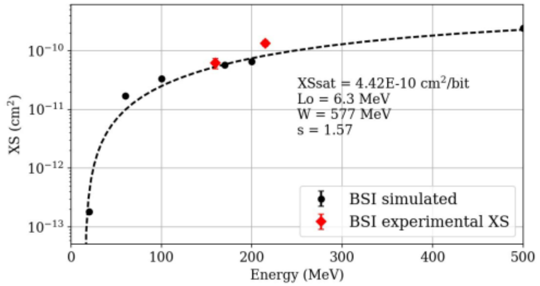

Fig. 7. Simulated SEL cross section for Brilliance.

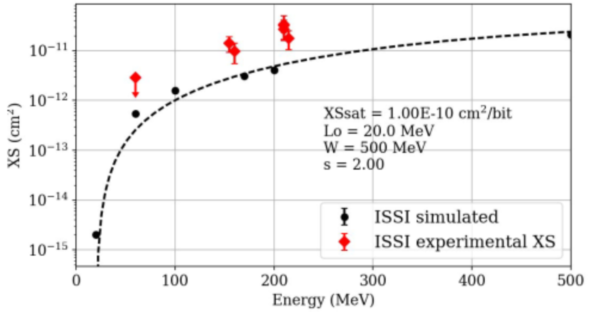

Fig. 8. Simulated SEL cross section for ISSI.

High-Energy Heavy Ions

V. Wyrwoll et al., "Longitudinal Direct Ionization Impact of Heavy Ions on See Testing for Ultrahigh Energies," in IEEE Transactions on Nuclear Science, vol. 67, no. 7, pp. 1530-1539, July 2020, doi: 10.1109/TNS.2020.2994370.

V. Wyrwoll et al., "Heavy Ion Nuclear Reaction Impact on SEE Testing: From Standard to Ultra-high Energies," in IEEE Transactions on Nuclear Science, vol. 67, no. 7, pp. 1590-1598, July 2020, doi: 10.1109/TNS.2020.2973591.

- Very High Energy (VHE, 100 MeV/n – 5 GeV/n) and Ultra High Energy (UHE, 5 GeV/n-150 GeV/n) ions will undergo nuclear reactions, undergoing fragmentation (high-energy projectile-like and fission products) and generating low-energy target-like recoils.

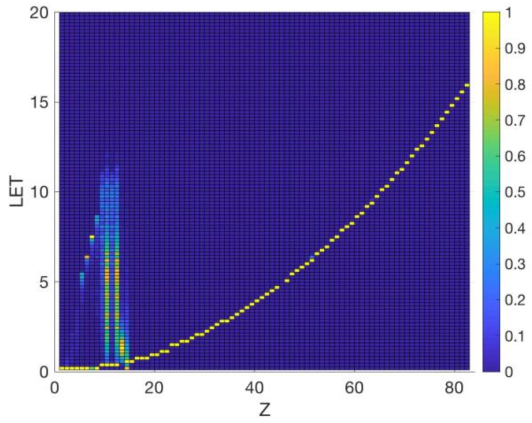

Fig. 8. FLUKA simulation of the LET spectra in a 140-μm silicon detector for 150-GeV/n ^{208}Pb without any material in front of the SV.

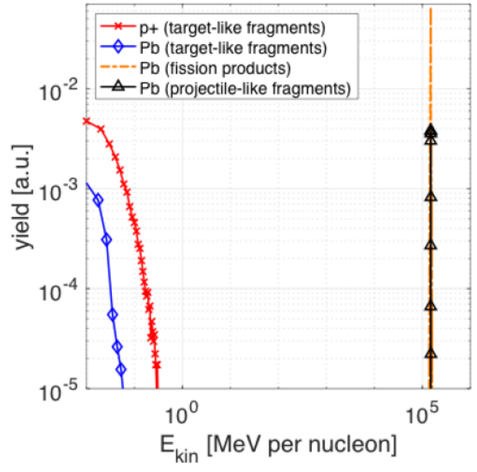

Fig. 9. Kinetic energy distribution of 150 GeV/n ^{208}Pb and 200 MeV protons on a 140 μm silicon target, focusing on target-like fragment, fission fragment and primary particle contribution.

Heavy ion SEE cross section in 10-100 MeV/n range

R. García Alía et al., "Sub-LET Threshold SEE Cross Section Dependency With Ion Energy," in IEEE Transactions on Nuclear Science, vol. 62, no. 6, pp. 2797-2806, Dec. 2015, doi: 10.1109/TNS.2015.2483021.

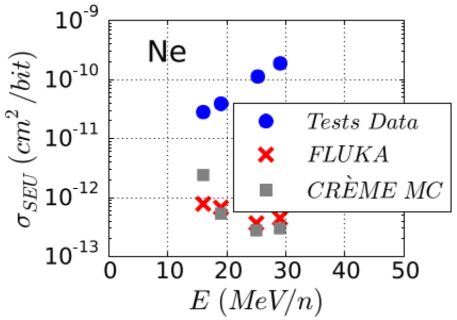

Fig. 8. Simulated SEU cross sections for Ne ions as a function of ion energy compared to experimental results.

- Monte Carlo codes predict relatively constant or decreasing heavy ion nuclear (i.e. sub-LET) SEE cross sections
- They also underestimate the experimental results, perhaps due to fragments generated in elements not considered in the simulation (e.g. collimators, vacuum windows)

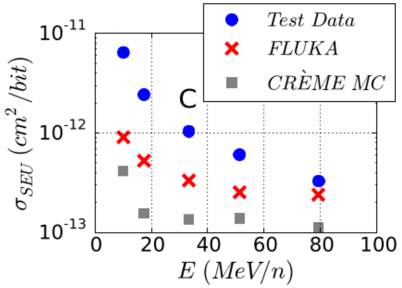

Fig. 7. Simulated SEU cross sections for C ions as a function of ion energy compared to experimental results.

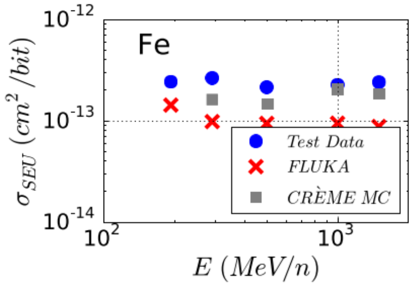

Fig. 6. Simulated SEU cross sections for Fe ions as a function of ion energy compared to experimental results.

Heavy ion vs. proton (indirectly energy deposition) SEE cross section

V. Wyrwoll et al., "Heavy Ion Nuclear Reaction Impact on SEE Testing: From Standard to Ultra-high Energies," in IEEE Transactions on Nuclear Science, vol. 67, no. 7, pp. 1590-1598, July 2020, doi: 10.1109/TNS.2020.2973591.

- Heavy ion nuclear SEE cross sections can be orders of magnitude larger than proton ones at low energy, but at high energy, they are only a factor a few larger

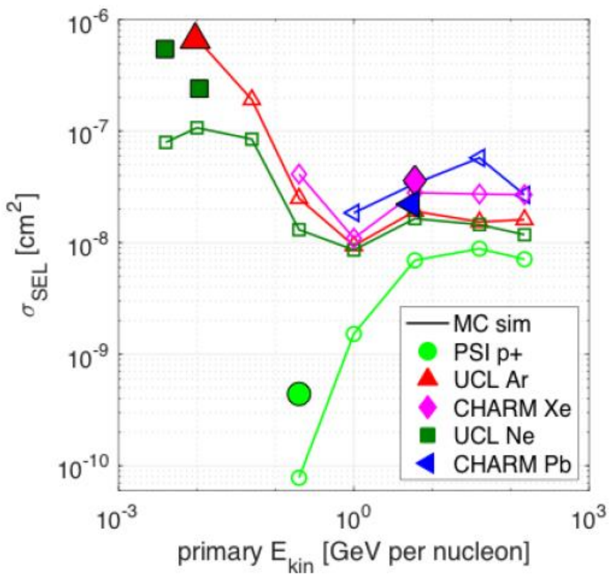

Fig. 12. FLUKA simulated sub-LET for heavy ions and proton SEL cross section as a function of ion energy for a SRAM memory up to 150 GeV/n compared to experimental data.

Solid state detector for energy deposition measurements

C. Cazzaniga et al., "Measurements of Low-Energy Protons using a Silicon Detector for Application to SEE Testing," in IEEE Transactions on Nuclear Science, doi: 10.1109/TNS.2021.3123814.

- Solid-state detector coupled to fast readout electronics, and calibrated through triple alpha source (and higher energy heavy ions, in cyclotron facilities)

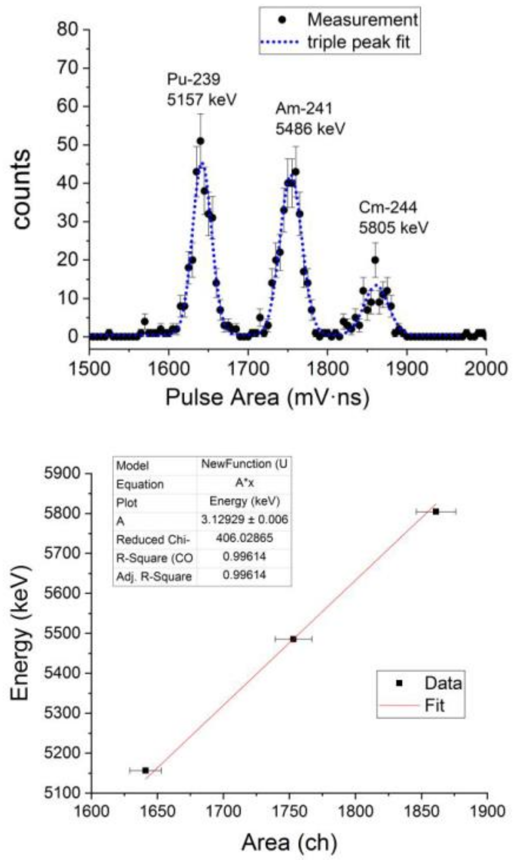

Fig. 5. Pulse area spectrum measured with a calibration triple-alpha source of ^{239}Pu, ^{241}Am and ^{244}Cm (top). Linear calibration of deposited energy as a function of pulse area (bottom).

Intermediate energy neutrons

D. Lucsányi, R. G. Alía, K. Biłko, M. Cecchetto, S. Fiore and E. Pirovano, "G4SEE: a Geant4-based Single Event Effect simulation toolkit and its validation through monoenergetic neutron measurements," in IEEE Transactions on Nuclear Science, doi: 10.1109/TNS.2022.3149989.

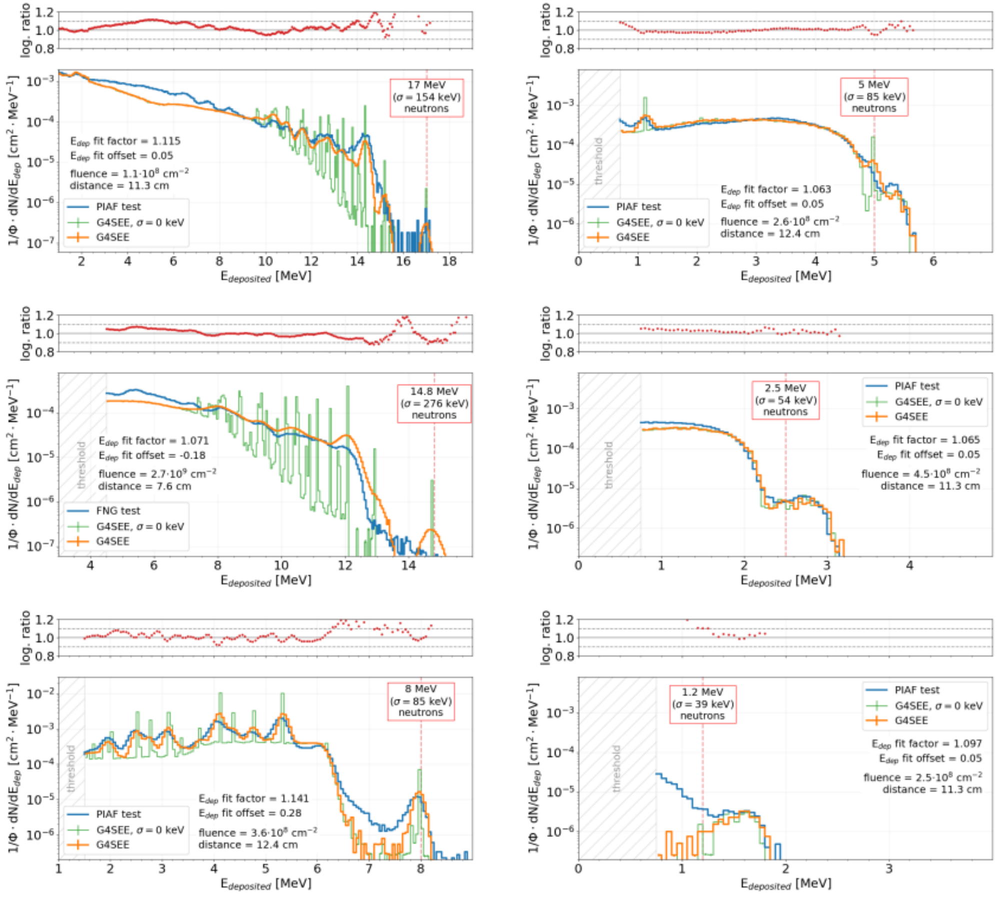

Fig. 7: Comparison of energy deposition distributions (fluence-normalized differential counts in function of deposited energy) measured with the diode at PIAF and FNG facilities (blue) and simulated using G4SEE (orange) with 17 MeV, 14.8 MeV, 8 MeV, 5 MeV, 2.5 MeV and 1.2 MeV neutrons. Simulated spectra with $\sigma_E = 0$ keV are also added (green). Logarithmic count ratios of measured and simulated distributions are plotted as well, showing the good agreement between them over several orders of magnitude.

- Energy deposition distribution in silicon for intermediate (0.2-20 MeV) energy neutrons

High-Energy Neutrons

CAZZANIGA, C., et al. Fast neutron measurements with solid state detectors at pulsed spallation sources. Journal of Neutron Research, 2020, vol. 22, no 2-3, p. 345-352.

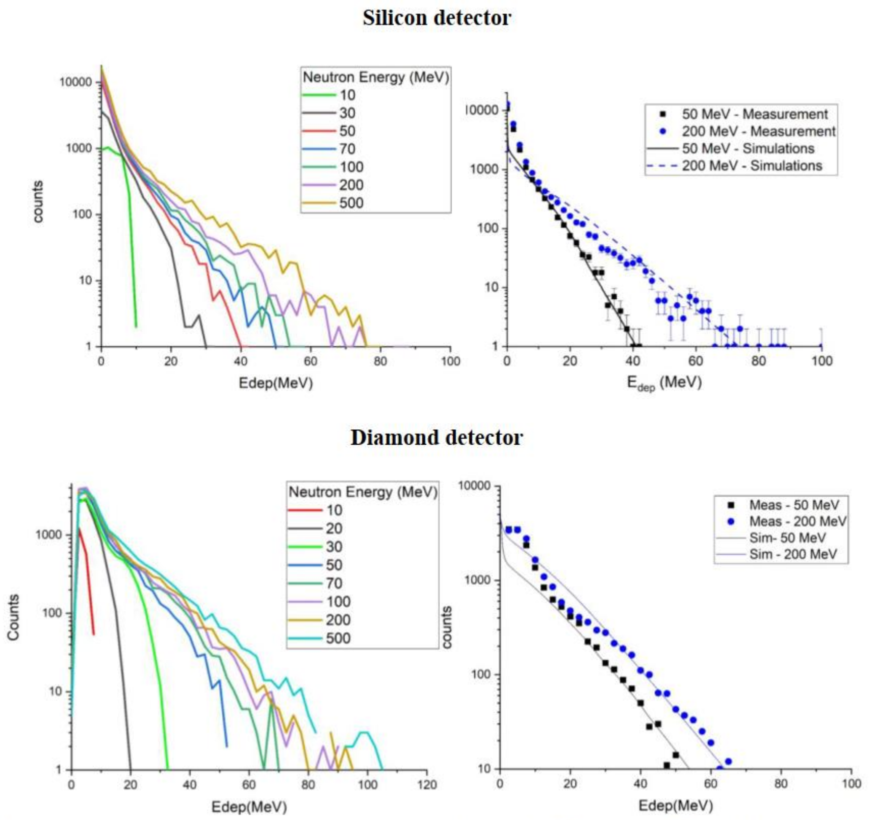

Figure 5. Fast neutron response functions as measured at nTOF (left). The right-hand panels show a subset of those measured response functions compared to FLUKA simulations. The upper panels are for the silicon detector and the lower panels are for the diamond detector.

- Energy deposition distribution in silicon for high (20-200 MeV) energy neutrons

High-Energy Protons

K. Bilko et al, “Silicon solid-state detectors for monitoring high-energy accelerator mixed field radiation environments”, RADECS 2021

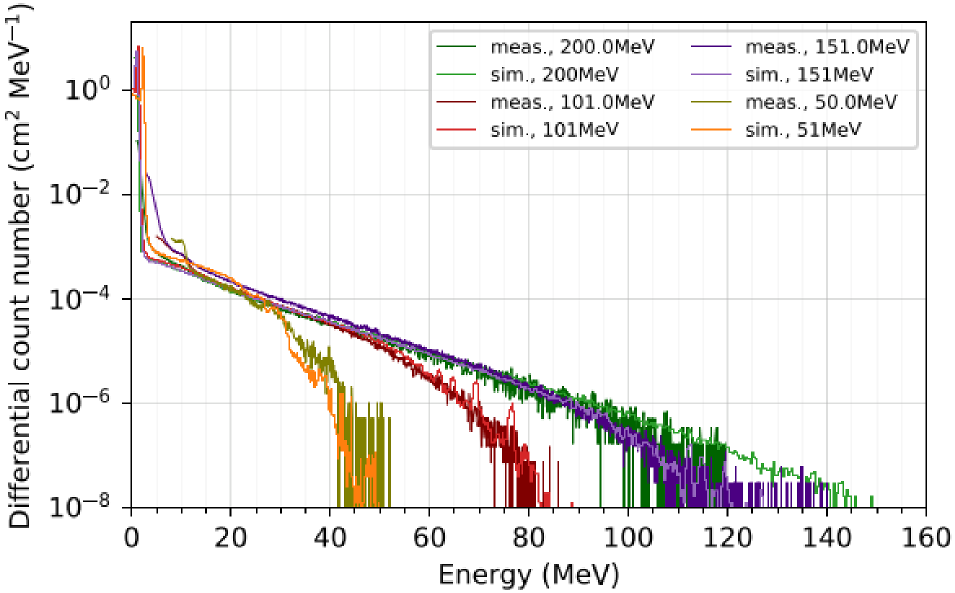

Fig. 4. Measured and simulated energy deposition spectra normalized with the proton fluence (for 1000 μm thick diode). Considered proton beam energies: 30, 51, 101, 151, 200 MeV, whereas 70 MeV is presented in Fig. 5.

- Energy deposition distribution in silicon for high (50-200 MeV) energy protons

Spallation neutron and mixed field

C. Cazzaniga, R. G. Alía, M. Kastriotou, M. Cecchetto, P. Fernandez-Martinez and C. D. Frost, "Study of the Deposited Energy Spectra in Silicon by High-Energy Neutron and Mixed Fields," in IEEE Transactions on Nuclear Science, vol. 67, no. 1, pp. 175-180, Jan. 2020, doi: 10.1109/TNS.2019.2944657.

- Mixed-field energy deposition measurements, and dominance of pions for high deposited energies

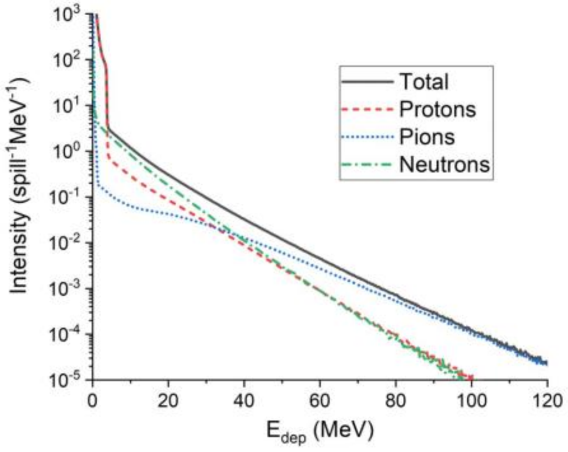

Fig. 5. FLUKA simulation of the deposited energy spectrum at CHARM separated for the contribution of neutrons, protons, and pions.

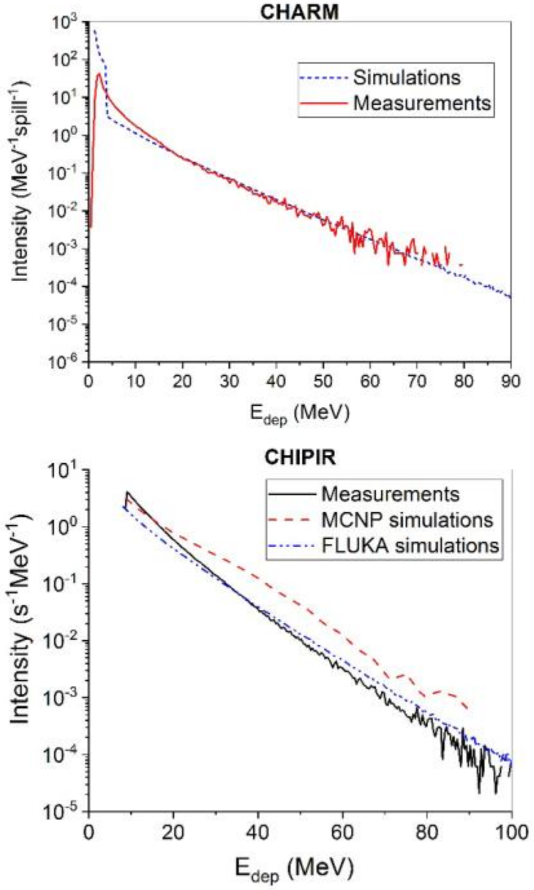

Fig. 2. Deposited energy spectra measured with a silicon detector at CHARM (top) and ChipIr (bottom). A comparison with Monte Carlo simulations of radiation transport is presented.

High-energy proton energy deposition distribution as a function of Monte Carlo code and nuclear model

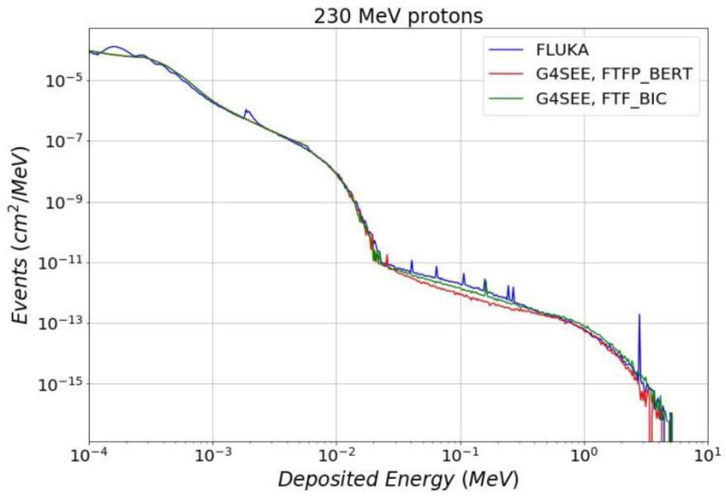

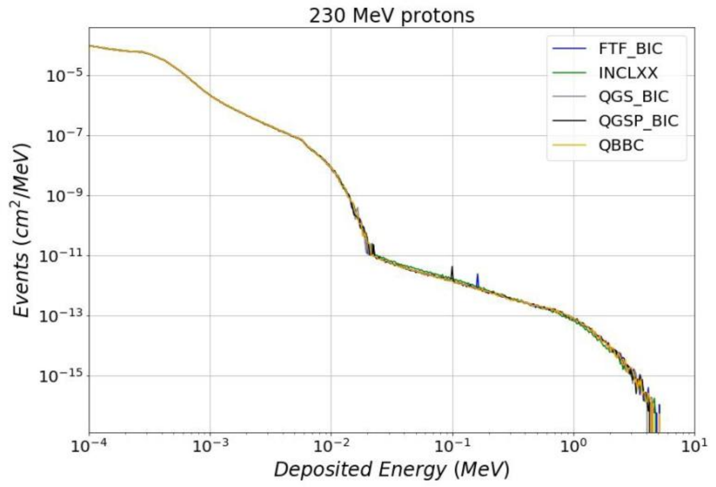

Spikes in energy deposition distribution are due to biasing – when integrated with the response function, their contribution to the total statistical error of the simulated SEU cross section is still within a few percent

Table 2: Simulated proton SEU cross sections for different physics model options, including the ratio with the experimental value in brackets.

Model	**230 MeV (10^{-14} cm^2/bit)**	**30 MeV (10^{-14} cm^2/bit)**
BERT	2.64 (1.04)	3.67 (1.48)
BIC	3.64 (1.43)	4.48 (1.81)
INCLXX	3.08 (1.21)	-
QGS_BIC	3.58 (1.41)	-
QGSP_BIC	3.62 (1.43)	-
QBBC	3.60 (1.42)	-
FLUKA	3.74 (1.47)	3.13 (1.26)

Conclusions and further thoughts

- Importance of benchmarking radiation effects simulations across different models and Monte Carlo codes, and against experimental data (*note: often not a direct comparison, due to uncertainties in SEE model parameters*)
- Solid state detectors provide a very useful means of directly comparing measured and simulated energy deposition distributions, but involve sensitive volumes that are much larger than those representative of SEEs (i.e. light, energetic secondaries dominate over heavy, high-LET, short-ranged)
- Comparison between FLUKA and different hadronic physics models in Geant4 for high-energy protons show differences that are relatively small (few tens of percent) when compared to other SEE model uncertainty sources (sensitive volume dimensions, surrounding materials, critical charge, etc.) but not completely negligible
- Differences in heavy ion nuclear reactions, both for the target-like and projectile/fission-like fragments, are expected to be larger and would require further assessment.

Thank you for
your attention!